Single-domain epitaxial silicene on diboride thin films

A. Fleurence,[1, a)] T. G. Gill,[1,2a,2b], R. Friedlein,[1,*] J. T. Sadowski,[3] K. Aoyagi,[1] M. Copel,[4] R. M. Tromp,[4] C. F. Hirjibehedin,[2a,2b,2c] and Y. Yamada-Takamura[1]

[1] *School of Materials Science, Japan Advanced Institute of Science and Technology (JAIST), 1-1 Asahidai, Nomi, Ishikawa 923-1292, Japan*

[2a] *London Centre for Nanotechnology, University College London (UCL), London WC1H 0AH, United Kingdom*

[2b] *Department of Chemistry, UCL, London, WC1H 0AJ, United Kingdom*

[2c] *Department of Physics & Astronomy, UCL, London WC1E 6BT, United Kingdom*

[3] *Center for Functional Nanomaterials, Brookhaven National Laboratory, Upton, New York 11973, USA*

[4] *IBM Research Division, Thomas J. Watson Research Center, Yorktown Heights, New York 10598, USA*

a) Corresponding author: antoine@jaist.ac.jp

[*] *present address: BU MicroSystems, Meyer Burger (Germany) AG, 09337 Hohenstein-Ernstthal, Germany*

Published as *Appl. Phys. Lett.* 108, 151902 (2016)

http://dx.doi.org/10.1063/1.4945370

Epitaxial silicene, which forms spontaneously on ZrB_2(0001) thin films grown on Si(111) wafers, has a periodic stripe domain structure. By adsorbing additional Si atoms on this surface, we find that the domain boundaries vanish, and a single-domain silicene sheet can be prepared without altering its buckled honeycomb structure. The amount of Si required to induce this change suggests that the domain boundaries are made of a local distortion of the silicene honeycomb lattice. The realization of a single domain sheet with structural and electronic properties close to those of the original striped state demonstrates the high structural flexibility of silicene.

Even though silicene and graphene share similar electronic properties[1], silicene differs from its carbon counterpart by the mixed sp^2/sp^3 hybridization of silicon atoms, which originates from its larger atomic radius. Exotic topological properties[2,3] and new functionalities[4] are expected to stem from the resulting buckled honeycomb structure of free-standing silicene. Experimentally, silicene has been found to exist only in epitaxial forms on a limited number of metallic substrates - including Ag(110)[5], Ag(111)[6–13], ZrB_2(0001)[14,15], Ir(111)[16], ZrC(111)[17] - and is stabilized by non-negligible interactions with the different substrates. These interactions cause variations in the atomic-scale buckling that are different from that of free-standing silicene. This structural flexibility allows epitaxial silicene to have a variety of structures with correspondingly different electronic properties.

Epitaxial silicene on the (0001) surface of ZrB_2 thin films grown on a Si(111) surface forms spontaneously by the self-terminating segregation of Si atoms from the silicon substrate[14]. The commensuration of the ($\sqrt{3} \times \sqrt{3}$) unit cell of the Si honeycomb lattice with the (2×2) unit cell of ZrB_2(0001) forces epitaxial silicene to be compressed by approximately 5 % with respect to the free-standing silicene and to adopt a specific buckling in such a way that the silicene is ($\sqrt{3} \times \sqrt{3}$)-reconstructed[14]. This reconstruction turns the Dirac cones into parabolic π-electronic bands separated by an electronic band gap[14,18]. Furthermore, this silicene sheet is systematically textured into a domain structure consisting of a highly ordered array of stripe domains[14,19] that density functional theory (DFT) calculations suggest occurs in order to avoid a phonon instability[20]. Epitaxial silicene formed on ZrB_2(0001) single crystal surface through Si deposition seems to have similar domain structure[15]. On the other hand, silicene formed on a ZrC(111) single crystal surface, which is more lattice-matching to free-standing silicene, seems to lack domain structure[15,17]. It is likely that the stripe domain structure has been introduced to reduce epitaxial stress. The formation of periodic domain structures that releases the stress of surfaces is also known to lower the free energy of the surfaces[21]. The robust structural flexibility of the silicene lattice may therefore be used to fine-tune its properties between different regimes. The regular striped domain structure of the silicene/ZrB_2 surface can be advantageously used to template linear chains of organic molecules[22], yet in other applications, such as those that utilize the transport properties of silicene[23] it may be more beneficial to produce domain-free surfaces.

In this Letter, we demonstrate that the epitaxial silicene with striped domain structure can be turned into a single-domain silicene sheet upon deposition of a small amount of Si atoms. The comparison of the structural and electronic properties between both silicene sheets indicates that the domain structure introduces very little change to the atomic structure. This is another demonstration of the structural flexibility of silicene, suggesting the possibility of tuning domain structure without altering its intrinsic properties.

ZrB_2(0001) thin films were grown on Si(111) by ultrahigh vacuum (UHV)-chemical vapor epitaxy, as described elsewhere[19]. Following the exposure to air and the transfer to separate UHV systems, silicene is generated by annealing for a few hours under UHV conditions at 800 °C[14]. The resulting surface consists of atomically flat few hundreds nm-wide terraces[19,24]. In order to determine the amount of Si in this spontaneously-formed silicene sheet in a precise and quantitative manner, medium-energy ion scattering (MEIS)[25] was carried out. The measurement used 100 keV protons, channeling in the [11$\bar{2}$3] direction of the ZrB_2(0001) thin film, while the backscattered protons were detected at a 70° scattering angle. The dynamic evolution of the surface structure during the deposition of Si atoms on the domain structure was investigated using the spectroscopic low-energy electron microscopy (Elmitec SPE-LEEM) end-station located at BL U5UA of the National Synchrotron Light Source (NSLS, Brookhaven National Laboratory, Upton, NY, USA). The change in surface structure upon Si deposition was also characterized by scanning tunneling microscopy (STM) and low-energy electron diffraction (LEED), performed at the authors' facilities. STM images were recorded at room temperature. In order to characterize the change in bonding and electronic structure upon Si deposition, core-level photoelectron spectroscopy and angle-resolved photoelectron spectroscopy (ARPES) were carried out at BL13B of the Photon Factory synchrotron radiation facility located at the High-Energy Accelerator Research Organization (KEK, Tsukuba, Japan), using photon energies ($h\nu$) of 130 eV and 43 eV, respectively. For ARPES, the total energy resolution was better than 35 meV as determined from the broadening of the Fermi level. At this end-station, the electric field vector of the light was at the fixed angle of 25° with respect to the photoelectron analyzer. In these experiments, Si atoms have been deposited using a well-outgassed, resistively heated Si wafer as a source.

The STM image shown in Fig. 1(a) is typical of spontaneously-formed epitaxial silicene covering the whole $ZrB_2(0001)$ thin film surface[14]. The $(\sqrt{3} \times \sqrt{3})$-reconstruction of silicene appears as a single protrusion per unit cell. In addition, a large-scale ordering is observed as stripe domains oriented along $ZrB_2\langle 11\bar{2}0\rangle$ directions. The same ordering is reflected in the LEED pattern shown in Fig.1(b) as the splitting of fractional spots into 6 different side spots. As shown in Fig. 1(d), this pattern is well reproduced by the Fourier transformation (FT) of the structure model depicted in Fig. 1(c), where each unit cell is represented by a Dirac function. The boundaries result from shifts of the size of a single $ZrB_2(0001)$ unit cell, along one of the $\langle 11\bar{2}0\rangle$ directions different from that of the stripe domain orientation. The width of the boundaries is then $L_b = (3\sqrt{3}/2)a$, where a is the lattice parameter of $ZrB_2(0001)$. The width of the domain is given by $L_d = N \times d$, where N is the number of $\langle 11\bar{2}0\rangle$ row of protrusions in the domain and $d = \sqrt{3}a$ is the distance along $\langle 1\bar{1}00\rangle$ between two successive rows. A good agreement between FT and LEED patterns is obtained for $N = 5$, which in the previous study[21] gave the lowest formation enthalpy.

The results of MEIS measurements on this surface are shown in Fig. 1(e). The channeling configuration used in this study efficiently suppresses the number of protons backscattering from Zr atoms in the deeper part of the film, and thus the Si peak at about 95 keV in Fig. 1(e) is well separated from the Zr peak at ~ 98 keV. The data can be fitted using the Molière scattering potential for both Si and Zr, and using standard calibration procedures for the absolute scattering intensities[25]. The best fit (shown by solid lines for both Si and Zr in fig. 2e), yields an areal density of Si atoms of $(1.77 \pm 0.08) \times 10^{15}$ cm^{-2} which corresponds to 1.02 ± 0.05 ML silicene assuming the honeycomb structure with a lattice constant of 3.65 Å[14].

Silicon deposition on this pristine silicene was monitored in real-time by LEEM operating in the μ-LEED mode using the 2-μm-selected-area aperture. The whole deposition sequence was carried out with a Si flux corresponding to 2 MLs of silicene per hour as calibrated using the contrast change in the dark field image of the Si(100) surface during the $(2 \times 1) \rightarrow (1 \times 2)$ transition upon Si deposition at the sample temperature of about 450 °C. Silicon depositions were repeated at several temperature on the domain structure surface, generated and regenerated after Si deposition by annealing at 800°C. The μ-LEED patterns shown in Fig. 2(a) were recorded prior to

(left side) and soon after the start of the deposition, upon which the splitting of the fractional spots totally disappeared (right side). This change was observed in the temperature range from 210 ˚C to 370 ˚C. The amount of Si required for the complete disappearance of the splitting as estimated from the deposition time was in between 3 % (60 seconds at 210 ˚C) and 5 % (90 seconds at 370 ˚C) of a silicene ML (1.73×10^{15} cm^{-2}), depending on the temperature. The disappearance of the splitting of the spots associated to the ($\sqrt{3} \times \sqrt{3}$) reconstruction suggests the gradual loss of ordering of the stripe domains. On the other hand, the constant position of the fractional spots indicates that the ($\sqrt{3} \times \sqrt{3}$) lattice parameter remains unchanged. As shown in Figs. 2(a) and 2(b), STM observations following the deposition of an amount of Si (at a higher deposition rate of ~1.5 ML/min.) slightly above the transition (approximately 0.1 ML) at 320 ºC show that the evolution of the LEED pattern is associated with the formation of a single-domain silicene layer while the surface reconstruction remains the same.

Core-level photoelectron spectra were recorded prior to and following the deposition of Si atoms. Silicon atoms were deposited in a stepwise manner until the splitting of the fractional spots in LEED pattern disappeared. The most relevant spectra are shown in Fig. 2(c): these are the spectrum of the as-grown silicene (black line) and of that obtained just after the disappearance of the splitting (red line). The former is very similar to those reported previously for epitaxial silicene on ZrB_2 thin films, which can be decomposed into three doublets associated with the three different environments experienced by the Si atoms in the ($\sqrt{3} \times \sqrt{3}$)-reconstructed unitcell[14,26]. At a glance, the spectrum recorded following the deposition of Si atoms appears to be almost unchanged. The spectra are dominated by two well-shaped doublets separated by 260 meV corresponding to the so-called “A” and “B” atoms sitting respectively on the hollow and near-bridge sites (see the inset figure of Fig. 2(c)). In the spectrum recorded before deposition, the full widths at half maximum (FWHM) are about 170 meV and 200 meV, respectively. After deposition, while the peak corresponding to “B” atom is at the same binding energy, that of the “A” atoms is shifted towards lower binding energy by about 20 meV. With the FWHM of about 150 meV and 170 meV, for the “A” and “B” components, respectively, both peaks become narrower after Si deposition. This might well be explained by the increased structural homogeneity once domain boundaries have been removed. The binding energy shift

related to the "A" atoms might indicate an increased valence electron density at these sites and/or could be related to a binding energy shift of the "C"-atomic component, which can only be estimated with fitting procedures[14,26].

The small change in core-level photoelectron spectroscopy results suggests a minor change in the buckling of the Si honeycomb layer. This is further demonstrated by the comparison of the ARPES results of silicene sheets with and without domain boundaries which are shown in Fig. 3. This result indicates that the domain boundaries are not affecting the intrinsic band structure of epitaxial silicene on $ZrB_2(0001)$ [14,18]. The influence of the structural changes on the low-energy electronic band structure of the surface is derived from the ARPES spectra obtained prior (Fig. 3(a)) and following (Fig. 3 (b), and (c) with guides to eye) the Si deposition.

As discussed previously[18], denoted X_2 and X_3 relate to bands with major contributions from Si p_z orbitals and minor ones from the Si s, p_x, and p_y. These states are therefore of partial π character. Non negligible hybridization with Zr d orbitals was found in the DFT calculation[18]. On the other hand, the feature marked as S_1 in the ARPES spectra is derived from a diboride surface state[14,18] that is almost completely composed of contributions from d orbitals of the outermost Zr layer[18].

When comparing the spectra in Figs. 3 (a) and (b), their close similarity is striking. This confirms that the structural changes are minor indeed and relate only to the rearrangements at the domain boundaries while the overall pattern of the local buckling is not affected. The spectra, and in particular features X_2 and X_3, obtained from the single-domain silicene sheet are, however, sharper than those from that with the domain structure. This is certainly related to a higher coherence of the electrons at low binding energies in electronic states with long-range order, while changes for S_1 are not as pronounced. Note that X_2 and X_3 shift slightly up by about 50 meV at the K point. This may be related to a change in the stress distribution within the Si network[27] associated to the vanishing of the domain structure.

The growth of single-domain silicene sheets on the $ZrB_2(0001)$ thin film surface indicates that, at least up to a few percent of a monolayer, Si atoms prefer to be incorporated into the domain boundaries of the pristine silicene layer. As suggested by theoretical considerations accompanied by first-principles calculations[21], the total

energy per Si atom increases such that the single-domain layer is not the ground-state of silicene on $ZrB_2(0001)$ surface. Accordingly, when the system is heated at temperatures high enough to reach its thermodynamic equilibrium, additional Si atoms are removed, and the domain structure recovers. In a similar manner, the amount of Si required to suppress the splitting of the fractional spots is higher for deposition at 370°C than for 210°C can be explained by the hindrance of Si incorporation into domain boundaries upon temperature increase, reflecting the metastable character of the single-domain silicene compared to the one with the domain structure.

The experimental results reported here show that in the range of coverage and temperature considered, this increase of total energy does not lead to the clustering of the additional Si atoms or to the formation of the proposed "dumbbell"[28] or "MoS_2-like"[29] structures.

The boundaries are made of a local distortion of the Si honeycomb structure such as the one proposed in ref. 20, and the density of Si atoms is locally decreased from 1.73 × 10^{15} cm^{-2} to 1.54 × 10^{15} cm^{-2}. Assuming that the vanishing of the splitting of the fractional spots in the LEED pattern corresponds to the completion of a monolayer and that at 210 °C, the trapping rate of the adatoms at the domain boundaries is close to 1, the amount of deposited Si atoms required to reach a monolayer corresponds to an averaged width of the domain of $N = 5.0 \pm 0.1$. This is in good agreement with the STM image in Fig. 1(a). Then, the corresponding areal density of Si atoms of the pristine silicene can be estimated to be 1.68 × 10^{15} cm^{-2}, which is in good agreement with the value determined by MEIS.

The incorporation of Si adatoms into domain boundaries involves two processes related to the movement of Si atoms: (i) the diffusion of adatoms to the boundaries and (ii) the collective displacement of all the atoms of at least one of the neighboring domains. The absence of Si islands on the surface suggests that the diffusion length of the Si adatoms is much larger than the distance between domain boundaries. The collective displacement of domains and the integration of adatoms at a boundaries might be the limiting processes of the formation of single-domain silicene.

In conclusion, we have demonstrated that a silicene sheet without domain structures

can be stabilized on ZrB_2(0001) thin films grown on Si wafers. This is done through depositing a slight amount of Si atoms on spontaneously formed epitaxial silicene. The required amount of Si atoms of less than 5 % of a ML verifies that the boundaries are created from a local distortion of the silicene honeycomb lattice. The stability of this single-domain epitaxial silicene sheet with structural and electronic properties very similar to that with stripe domains indicates that the domain structure is not a requisite to stabilize silicene on ZrB_2(0001), but is introduced to lower the total energy per Si atom. This highlights the remarkable structural flexibility of epitaxial silicene to accommodate substrate-induced stress, which makes a vivid contrast to rigid graphene.[30]

We are grateful for experimental help from K. Mase (Institute of Materials Structure Science, High Energy Accelerator Research Organization, Tsukuba, Japan) and A. Al-Mahboob (CFN, BNL). Part of this work has been performed under the approval of the Photon Factory Advisory Committee (Proposal No. 2012G610). This research used resources of the Center for Functional Nanomaterials and National Synchrotron Light Source, which are the U.S. DOE Office of Science User Facilities, at Brookhaven National Laboratory under Contract No. DE-SC0012704. This work was supported by JSPS KAKENHI Grant numbers 26790005 and 26246002. AF acknowledges financial support from Asahi Glass Foundation; TG and CFH from the UK Engineering and Physical Sciences Research Council (EP/H026622/1 and EP/G036675/1).

REFERENCES

1. S. Cahangirov, M. Topsakal, E. Akturk, H. Sahin, and S. Ciraci, Phys. Rev. Lett. **102**, 236804 (2009).

2. M. Ezawa, New J. of Physics **14**, 033003 (2012).

3. M. Ezawa, Phys. Rev. Lett. **110**, 026603 (2013).

4. W.-F. Tsai**,** C.-Y. Huang, T.-R. Chang, H. Lin, H.-T. Jeng and A. Bansil, Nat. Commun. **4**, 1500 (2013).

5. P. De Padova, C. Quaresima, P. Perfetti, B. Olivieri, C. Leandri, B. Aufray, S. Vizzini, and G. Le Lay, Nano Lett. **12**, 5500 (2012).

6. C.-L. Lin, R. Arafune, K. Kawahara, N. Tsukahara, E. Minamitani, Y. Kim, N. Takagi, and M. Kawai, Appl. Phys. Express **5**, 045802 (2012).

7. B. Feng, Z. Ding, S. Meng, Y. Yao, X. He, P. Cheng, L. Chen, and K. Wu, Nano Lett. **12**, 3507 (2012).

8. H. Jamgotchian, Y. Colignon, N. Hamzaoui, B. Ealet, J. Y. Hoarau, B. Aufray and J. P. Bibérian, J. Phys.: Condens. Matter. **24**, 172001 (2012).

9. D. Chiappe, C. Grazianetti, G. Tallarida, M. Fanciulli and A. Molle, Adv. Mater. **24**, 5088 (2012).

10. P. Vogt, P. De Padova, C. Quaresima, J Avila, E. Frantzeskakis, M. C. Asensio, A. Resta, B. Ealet, and G. Le Lay , Phys. Rev. Lett. **108**, 155501 (2012).

11. L. Chen, C.-C. Liu, B. Feng, X. He, P. Cheng, Z. Ding, S. Meng, Y. Yao, and K. Wu, Phys. Rev. Lett. **109**, 056804 (2012).

12. L. Chen, H. Li, B. Feng, Z. Ding, J. Qiu, P. Cheng, K. Wu, and S. Meng, Phys. Rev. Lett. **110**, 085504 (2013).

13. P. De Padova, P. Vogt, A. Resta, J. Avila, I. Razado-Colambo, C. Quaresima, C. Ottaviani, B. Olivieri, T. Bruhn, T. Hirahara, *et al*., Appl. Phys. Lett. **102**, 163106 (2013).

14. A. Fleurence, R. Friedlein, T. Ozaki, H. Kawai, Y. Wang, and Y. Yamada-Takamura, Phys. Rev. Lett. **108**, 245501 (2012).

15. T. Aizawa, S. Suehara and S. Otani, J. Phys.: Condens. Matter **27**, 305002 (2015).

16. L. Meng, Y. Wang, L. Zhang, S. Du, R. Wu, L. Li, Y. Zhang, G. Li, H. Zhou, W. A. Hofer, *et al*., Nano Lett. **13**, 685 (2012).

17. T. Aizawa, S. Suehara and S. Otani, J. Phys. Chem. C **118**, 23049 (2014).

18. C.-C. Lee, A. Fleurence, Y. Yamada-Takamura, T. Ozaki, and R. Friedlein, Phys. Rev B **90**, 075422 (2014).

19. Y. Yamada-Takamura, F. Bussolotti, A. Fleurence, S. Bera, and R. Friedlein, Appl. Phys. Lett. **97**, 073109 (2010).

20. C.-C. Lee, A. Fleurence, R. Friedlein, Y. Yamada-Takamura, and T. Ozaki, Phys. Rev B, **90**, 241402 (2014).

21. O. L. Alerhand, D. Vanderbilt, R. D. Meade, and J.D. Joannopouolos, Phys. Rev. Lett. **61**, 1973 (1988).

22. B. Warner,T. G. Gill, A. Fisher,A. Fleurence, Y. Yamada-Takamura, and C. F. Hirjibehedin, to be submitted.

23. L. Tao, E. Cinquanta, D. Chiappe, C. Grazianetti, M. Fanciulli, M. Dubey, A. Molle and D. Akinwande, Nature Nanotech. **10**, 227 (2015).

24. A. Fleurence, W. Zhang, C. Hubault, Y. Yamada-Takamura Appl. Surf. Science **284**, 432 (2013).

25. J. F. van der Veen, Surface Science Reports **5**, 199 (1985).

26. R. Friedlein, A. Fleurence, K. Aoyagi, M. P. de Jong, H. Van Bui, F. B. Wiggers, S. Yoshimoto, T. Koitaya, S. Shimizu, H. Noritake, *et al*., J. Chem. Phys. **140**, 184704 (2014).

27. Y. Wang and Y. Ding, Solid State Commun. **155**, 6 (2013).

28. V. Ongun Ozcelik and S. Ciraci, J. Phys. Chem. C **117**, 26305 (2013).

29. F. Gimbert, C.-C. Lee, R. Friedlein, A. Fleurence, Yukiko Yamada-Takamura, and T. Ozaki, Phys. Rev. B **90,** 165423 (2014).

30. J. C. Meyer, A. K. Geim, M. I. Katsnelson, K. S. Novoselov, T. J. Booth, and S. Roth, Nature **446**, 60 (2007).

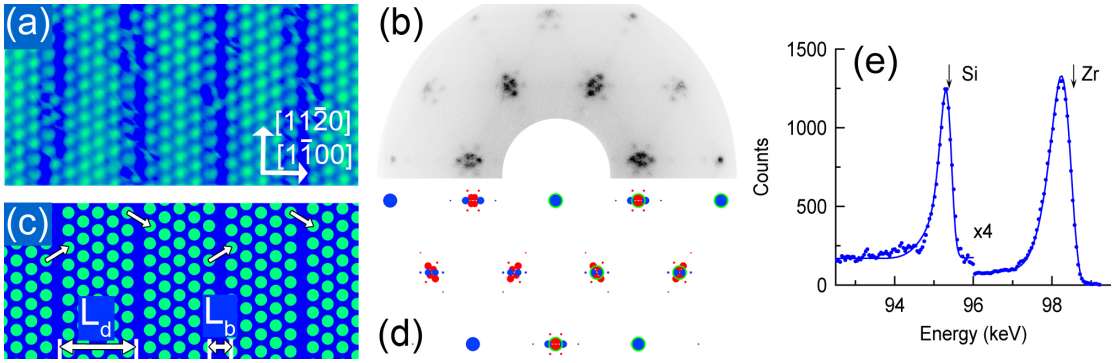

Figure 1. Pristine silicene on ZrB_2(0001). (a) STM image (14 nm × 7 nm, V = 1.0 V, I = 50 pA). (b) LEED pattern (E = 40 eV). (c) The model domain structure with N=5. (d) Fourier Transform of (c). Blue and red spots correspond to the structure of panel (c) and to the two other equivalent orientations, respectively. The size of the spots correlates with their intensity and the green dots on the right side indicate the expected positions of the diffraction spots of a domain-fee silicene with the same lattice parameter. (e) Measured (dots) and simulated (line) MEIS spectra for pristine silicene on ZrB_2 thin film.

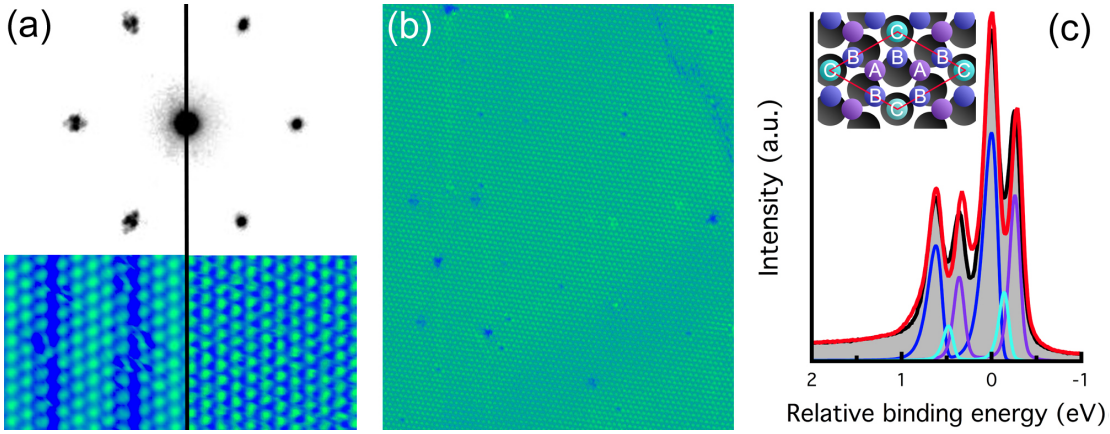

Figure 2. (a) μ-LEED (E = 30 eV) and STM images (7 nm × 7 nm, V = 1.0 V, I = 50 pA) recorded before (left panel) and after (right panel) the formation of single-domain silicene. (b): STM image (40 nm × 50 nm, V = 1.0 V, I = 50 pA) of epitaxial silicene after 0.1 ML Si deposition. (c) Si 2*p* core-level spectra before (black line, grey-filled) and after (red line) the deposition of Si atoms. Result of curve fitting for pristine silicene considering Si atoms in three different environments (inset figure: A, B, and C) are shown in purple (A), dark blue (B), and light blue (C) lines[26].

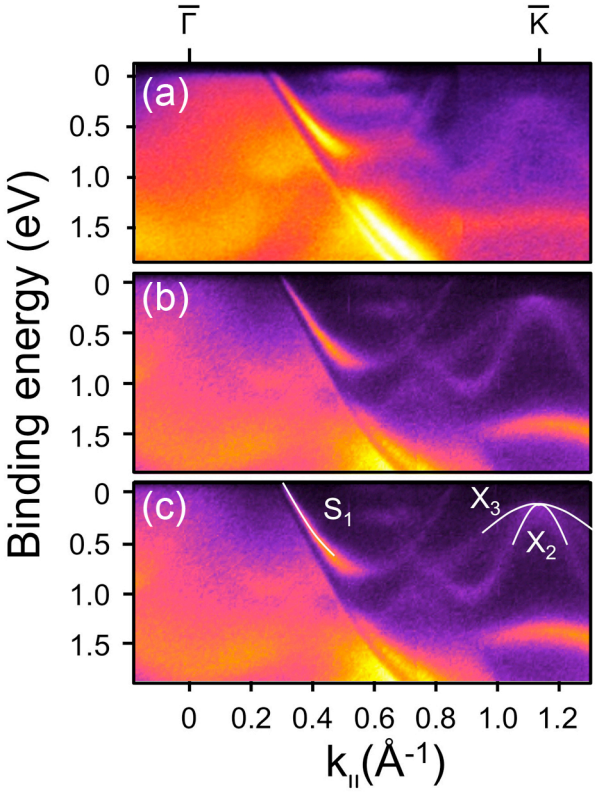

Figure 3. ARPES spectra (a) before and (b) after Si deposition on pristine silicene. Spectrum in (c) is the same as (b), with high-symmetry points related to (1×1)-silicene indicated.